INJECTION BEAM DYNAMICS IN SPEAR3*

J. Corbett[1], W. Cheng[2], A.S. Fisher[1], X. Huang[1], W. Mok[3], J. Safranek[1] and S. Westerman[1]

[1]SLAC National Accelerator Laboratory, Menlo Park, CA 94025
[2]Brookhaven National Laboratory, Upton, NY 11973
[3]Life Imaging Technology, Palo Alto, CA 94301

Abstract

For the top-off operation it is important to understand the time evolution of charge injected into the storage ring. The large-amplitude horizontal oscillation quickly filaments and decoheres, and in some cases exhibits non-linear x-y coupling before damping to the stored orbit. Similarly, in the longitudinal dimension, any mis-match in beam arrival time or beam energy results in damped, non-linear synchrotron oscillations. In this paper we report on measurements of injection beam dynamics in the transverse and longitudinal planes using turn-by-turn BPMs, a fast-gated, image-intensified CCD camera and a Hamamatsu C5680 streak camera.

INTRODUCTION

SPEAR3 is a 3rd generation, 3GeV storage ring light source with nominal emittance ε_x=10nm-radian. Single-bunch top-off injection occurs at either 8 hr or 10 min intervals with photon beamline shutters open [1]. Since the injector and BTS transport line were not specifically designed for top-off, it is particularly important to measure and understand dynamics of the injected beam in order to minimize perturbations seen by the users and to protect sensitive ID magnets in the lattice.

The injection system consists of a 10Hz booster synchrotron with single-bunch filling capability. Under nominal I=200mA operating conditions each stored bunch contains ~550pC. Each injected pulse contains ~30pC.

A number of diagnostic instruments are used to measure the injected beam dynamics. Centroid motion is monitored with fast turn-by-turn BPMs developed specifically for SPEAR3 [2]. Optical imaging of the charge distribution is possible at a diagnostic beam line which directs 3.5 x 6mrad of unfocused visible/UV light to an optical bench. After passing through a 6" diameter, f=2m collection lens the light is relayed to one of several diagnostic stations. An intensified, fast-gated camera can image the transverse beam profile at each turn but the light intensity is low and in most cases must be averaged over consecutive injection events [3]. Similarly, in the longitudinal direction, a dual-axis streak camera can be used to image the injected beam profile by integrating over a series of injection pulses [4].

As reported in [5], a systematic program was carried out to optimize electron beam steering and lattice optics through the booster-to-SPEAR (BTS) transport line. Important elements of this work included removal of stainless steel windows intercepting the beam path and application of response-matrix analysis to correct the beam optics.

For injected-beam measurements, the incoming single-bunch charge is only ~30pC and turn-by-turn BPM resolution is only about 1mm. As a result, horizontal injection oscillations can be resolved but small amplitude vertical motion and synchrotron oscillations require averaging. In order to measure the injected pulse dynamics at each injection cycle injection kicker #3

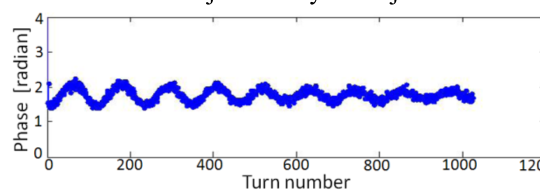

Figure 1: Synchrotron oscillations on the beam centroid due to booster/SPEAR timing mis-match.

(downstream of the injection septum) is triggered at the nominal injection time while injection kickers #1 and #2 (upstream of the septum) are mis-matched and triggered 50ms late to kick out the stored beam.

Of particular interest, the synchrotron oscillation component was extracted via FFT processing and the initial phase-space coordinates of the motion used to match injected beam energy and timing. An example where the injection beam is phase mis-matched is illustrated in Fig. 1. In this case the synchrotron oscillation amplitude is large, about 1 radian in rf phase. At 781ns per turn, the ~125 oscillation period agrees well with the nominal 10kHz synchrotron oscillation frequency. Although the beam arrival time can be adjusted manually, the phase drift typically requires adjustment several times per day.

TRANSVERSE BEAM DYNAMICS

A fast-gated, MCP-intensified PiMax camera was used to image the transverse profile of the beam at injection. Visible light focused through a commercial 1:5 lens onto the front-end photocathode yields a net de-magnification of M=0.59. A parallel optical path uses a combination of single-plane cylindrical lenses to yield a net de-magnification of M_x=0.7 and M_y=0.2 in the x/y planes, respectively [3,6]. In both cases the SR light passes through a vertical corner-periscope to create a 90 degree coordinate rotation. The horizontal beam axis and horizontal betatron motion are then oriented perpendicular

*Work sponsored by U.S. Department of Energy Contract DE-AC03-76SF00515 and Office of Basic Energy Sciences.
[1]corbett@slac.stanford.edu

to the optical bench and along the vertical axis of the camera CCD. For the injected beam, with all filters removed, each turn yields a few thousand photons per pass across the UV/visible camera detection bandwidth [7]. As the beam filaments the photon flux is spread out over more pixels and the image becomes increasingly difficult to detect.

To enhance contrast, the PiMax software is configured to take multiple exposures of a single turn over a series of injection pulses. Light from ten's of separate injection

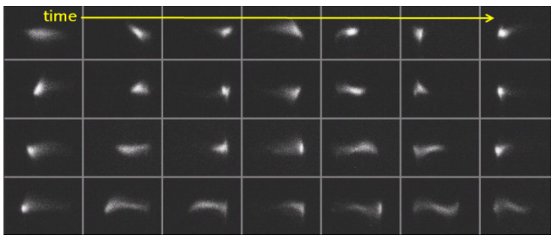

Figure 2: Transverse images of injected beam. Coordinate rotations corrected in software.

events is integrated on the CCD chip to produce a single camera 'frame' before readout and advance to the next frame. The software *sequence* mode is used to set the frame exposure count and advance from turn-to-turn as the booster injects beam into SPEAR3. As described above, the charge from each injected pulse is ejected using mis-timed kickers prior to the next injection cycle.

Figure 2 shows an example of the multi-exposure, multi-turn imaging technique utilizing the 1:5 lens branch line (no rotating mirror). The left/right motion is due to the inherent horizontal betatron oscillation in the injected beam and up/down motion indicates some degree of coupling. Each image represents a transverse projection of the charge distribution on a turn-by-turn basis. At the extremes in horizontal position the charge distribution appears as a relatively tight spot while exposures taken as the charge passes across the center of the screen generate 'comet-like' images.

One plausible explanation is that tune shift with betatron amplitude leads to charge filamentation. Other possible causes include chromaticity with energy spread and tumbling of a mis-matched beam as it rotates in phase-space. Either way, the camera only sees images projected onto the x-axis from the full x-x' phase space distribution.

In a more complete scenario each image can be viewed as an x-y projection of the 3-D bunch structure or 'snake' of injected charge moving toward the observer. A full account of the transverse turn-by-turn images must then take into account evolution of the vertical and longitudinal charge distribution in time.

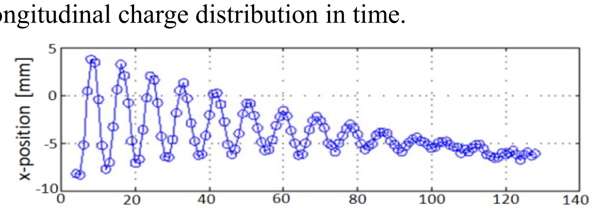

Figure 3: BPM measurement of the injected beam centroid in the horizontal plane.

One consequence of charge filamentation is the appearance of rapid damping of the beam centroid as seen by the BPMs. Hence, as illustrated in Fig. 3, the nominal 3500-turn damping time can be masked by non-linear filamentation of the injected charge.

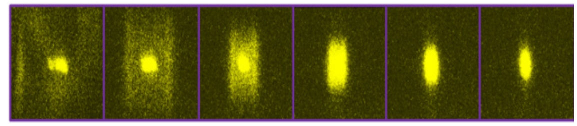

Figure 4: Injected charge distribution every 2ms.

Further into the injection process, the charge distribution continues to smear in the x-y plane until the photon flux density becomes so low that details are difficult to resolve. The time sequence displayed in Fig. 4 shows how after a several damping times, the injected charge re-coalesces to the closed-orbit beam axis. Here, starting at t=100μs, the time evolution of injected charge is captured every 2ms, and the rf voltage was lowered to the level where only a few μA of charge remains to mark the stored beam axis but does not accumulate. For each exposure the camera gate was held open for 5μs. Although the charge couples into the vertical plane the injected charge capture efficiency is known to approach 100% under optimal injection conditions.

LONGITUDINAL BEAM DYNAMICS

In terms of longitudinal coordinates, the injected beam is captured and damped in the non-linear potential of the rf system. Ideally the injected charge is matched in arrival time (synchronous phase), distribution in arrival time, average beam energy and energy spread. This section investigates injected beam dynamics in the longitudinal plane for long- and short timescales. In each case the Hamamatsu C5680 streak camera is used to collect data in dual-scan mode.

Since precise measurements of bunch length are not required here and the radiated light intensity is often low,

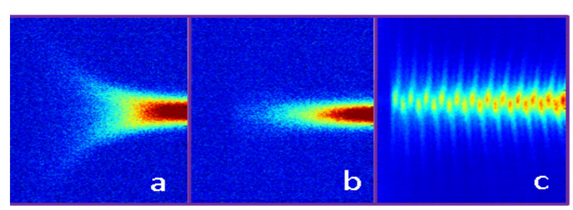

Figure 5: Dual-scan streak camera image of injected beam on 10ms and 1ms time scales.

no optical filters are used. The signal is integrated on the camera CCD using the inject/kickout scheme described above. The vertical time scale for the R2 synchroscan is 704ps full scale or 0.69ps-per-pixel.

Starting with long time scale injection phenomena, Fig. 5 shows beam capture with (a) injection phase mis-match and (b) correct timing during the first 10ms of injection ($\tau_{||,damp}$=2.8ms). The initial large-amplitude oscillations are not visible with correct timing. Figure 5-c zooms in to the 1ms time scale to illustrate the presence of 10kHz synchrotron oscillations, even with accurate injection timing. Figure 6 shows the same injected charge sequence during the first 3.5ms, in this case rendered from a series of seven 500µs horizontal-sweep images stacked together in software.

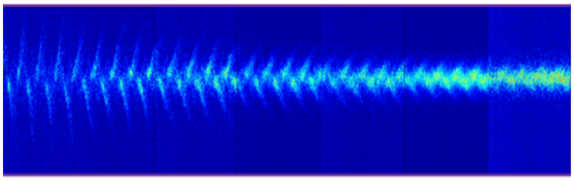

Figure 6: Evolution of longitudinal bunch distribution during first 3.5ms after injection.

Similar to motion in the transverse plane, time evolution of the bunch in the longitudinal dimension can be influenced by filamentation and rotation of the bunch distribution in phase-space. Filamentation is caused by synchrotron tune shift with amplitude in the non-linear rf potential. In the damped condition the stored beam typically executes ~1ps rms coherent synchrotron oscillations.

By adjusting the injected beam arriving time, one can see the longitudinal beam dynamics with timing mis-match, as shown in Fig. 7. In first four plots to the left the horizontal sweep time is 1ms, vertical synchroscan range is R2 (704ps) and the delay times are 0, 20, 30 and 45ps relative to synchronous injection. From these images it is clear that filamentation and/or phase-space mis-match cause the charge to disperse over a range of time much greater than the bunch centroid delay time. The motion shown furthest to the right was taken in R4 synchroscan mode has 150ps injection delay. In this case the vertical time scale is 1687ps and the injected bunch exhibits coherent dipole-mode oscillations.

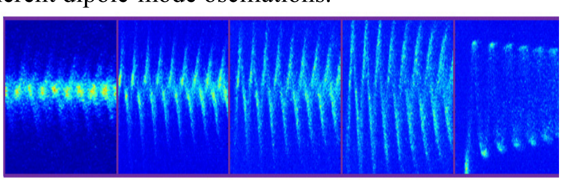

Figure 7: Longitudinal injection oscillations with arrival time error Δt=0, 20, 30, 45 and 150ps (R4).

If we now zoom in to short-time dynamics, Fig. 8-a shows clear evidence of phase-space mismatch in the injected beam. The projected charge density as seen by the streak camera periodically appears as a 'condensed' image and a 'diffuse' image alternating at twice the synchrotron frequency as the distribution rotates in phase-space. In the 'diffuse' projection the bunch length is found to be several hundred ps long. The corresponding energy spread can be extracted from the 'condensed' state. A good description of these phenomena with a comparison to simulation is given in [8].

In Figure 8-b the horizontal time scale is further reduced to 50µs so that initially the injected bunch can be resolved on a turn-by-turn basis in 2-D x-t coordinates. The small tilt or x-t correlation is indicative of charge dispersion in the horizontal plane as seen on the PiMax camera. After about 10 turns, a more complete de-coherence is evident. Of note, the images in Fig. 8 were integrated over 30 injection pulses, demonstrating a high level of injector stability over short time intervals.

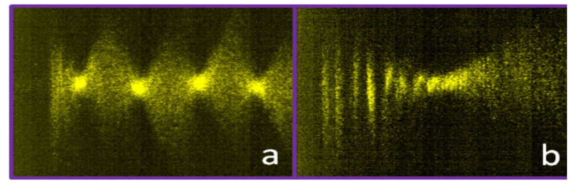

Figure 8: Evolution of charge injected bunch distribution on (a) 200µs and (b) 50µs time scales.

In order to further resolve turn-by-turn beam dynamics the optical beam transport line leading to the streak camera was modified to incorporate cylindrical lenses. A weak horizontal lens was used in conjunction with a strong vertical lens to produce magnification in the horizontal direction and de-magnification in the vertical direction. The small vertical spot size is necessary for good time resolution. By rotating the incoming beam with a dove prism, the bunch can be imaged in the y-t plane. In conjunction with the PiMax camera, the object was to capture a full rendering of the bunch in x-y-t coordinates.

SUMMARY

For top-off operation the incident charge must be well matched in the transverse and longitudinal dimensions for efficient capture, radiological concerns and ID protection. Turn-by-turn BPMs are used to control the 6-D launch conditions into the storage ring. Synchrotron light diagnostics are used to monitor different projections of the charge distribution. The fast-gated camera shows evidence of filamentation in the horizontal plane caused by tune shift with betatron amplitude and/or optical mis-match. In the longitudinal plane the correct timing, beam energy and phase-space distribution are needed to minimize turbulence in the rf bucket.

REFERENCES

[1] J. Schmerge, *et al*, "Summary report on SPEAR3 top-off injection safety", SSRL-AP-007, 2009.

[2] J. Sebek, *et al*, "Design and performance of SSRL beam position electronics", BIW10, (2010).

[3] W. Cheng, *et al*, "Fast-gated camera measurements in SPEAR3", PAC09, Vancouver, Canada, (2009).

[4] W.Cheng, A.S.Fisher and J.Corbett, "Streak camera measurements in PEP-II and variable optics in SPEAR3", BIW08, Lake Tahoe, CA (2008).

[5] J. Safranek, *et al*, "Optimization of the booster to SPEAR3 transport line for top-off injection", PAC09, Vancouver, Canada (2009).

[6] A.S. Fisher, *et al.*, "Turn-by-turn imaging of the transverse beam profile in PEP-II", BIW06, Batavia, IL, (2006).

[7] J. Corbett, *et al*, "Visible light diagnostics at SPEAR3", SRI09, Melbourne, Australia (2009).

[8] J. Byrd and S. De Santis, "Longitudinal injection transients in an electron storage ring", PRST-AB, Vol. 4, 024401 (2001).